CHROMATICITY COMPENSATION – MAIN INJECTOR SEXTUPOLE STRENGTH

S.A. Bogacz and S. Peggs

Accelerator Physics Department,
Fermi National Accelerator Laboratory*
P.O. Box 500, Batavia, IL 60510

April 1991

The current Main Injector lattice is studied in the context of full chromaticity compensation in the presence of eddy current, saturation and static sextupole fields generated by the dipole magnets. Two families of correcting sextupole magnets are placed to compensate these fields and to adjust the chromaticity (in both planes) to some desired value. Variation of the dipole induced sextupole fields with the B-field (changing along a ramp) are modelled according to recent experimental measurements of the Main Injector dipole magnet. Analysis of the required sextupole strengths is carried out along two realistic momentum ramps. The results of our calculation give quantitative insight into the requisite performance of the sextupole magnets.

*Operated by the Universities Research Association, Inc., under a contract with the U.S. Department of Energy

INTRODUCTION – MAIN INJECTOR LATTICE

Before we proceed with the chromaticity compensation analysis a brief overview of a current Main Injector lattice and its basic features is in place. The mi_17 Main Injector lattice is made up of three kinds of cells depicted schematically in Figure 1 (54 "regular" cells, 32 "dispersion suppressor" cells and 18 "empty" cells). These cells can be described as follows: the regular cell – a slightly detuned FODO cell containing four dipole and two quadrupole magnets per cell, the empty cell – a regular cell with removed dipoles and finally the dispersion suppressor cell – a cell shorter by factor of 3/4 than the regular cell with the dipole magnets shortened by factor 2/3 and the quadrupoles elongated by factor of 4/3 (with respect to the corresponding magnet lengths in the regular cell). The locations of other elements like the dipole correctors, trim quads, beam position monitors and sextupole magnets are also illustrated in Figure 1. The Main Injector lattice is constructed to have two-fold symmetry. Half of the lattice along with the twiss functions is illustrated in Figure 2. Introduced into the lattice dispersion suppressing mechanism can be seen by looking at the horizontal dispersion function plotted in Figure 2. The following simple numerology,

$$\frac{3}{4}\times\frac{2}{3}=\frac{1}{2}\ , \tag{1}$$

assures zero horizontal dispersion at the appropriate lattice locations – an important feature of the discussed lattice.

The lattice is tuned to the horizontal tune of 26.4 and the vertical tune of 25.4. The final tuning was done through adjustment of the dispersion suppressor cell length, while its focusing end defocusing quadrupoles match the corresponding quadrupole strengths in the regular cell.

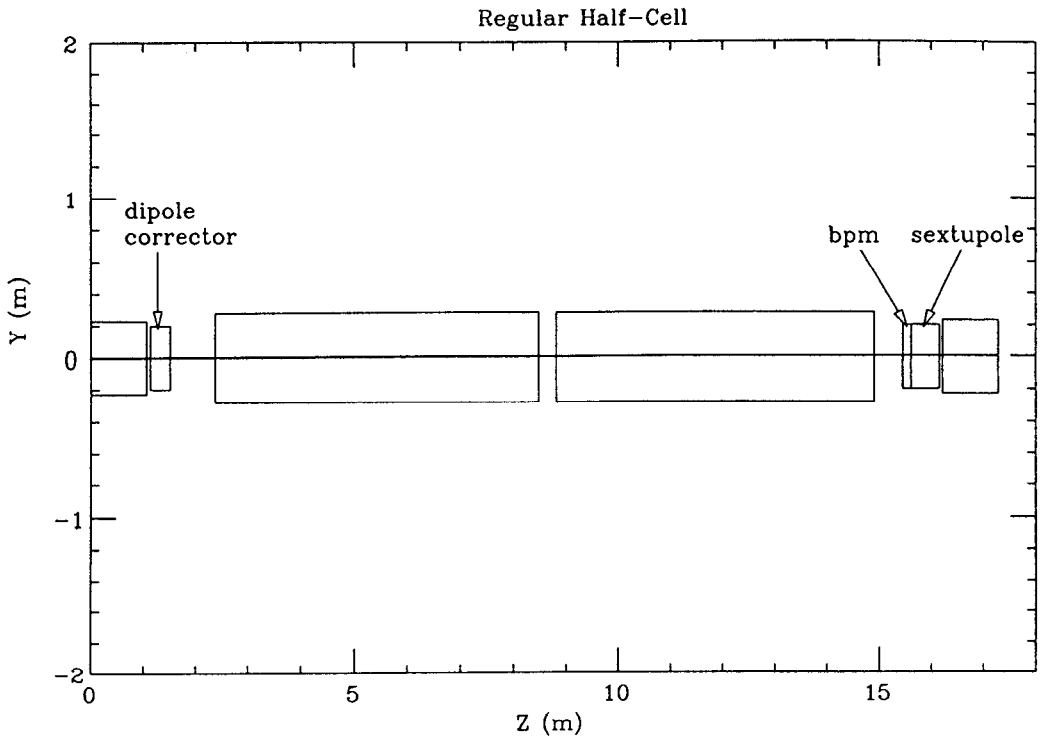
Regular Half-Cell
dipole
corrector
bpm
sextupole
Y (m)
Z (m)
2
1
0
-1
-2
0
5
10
15

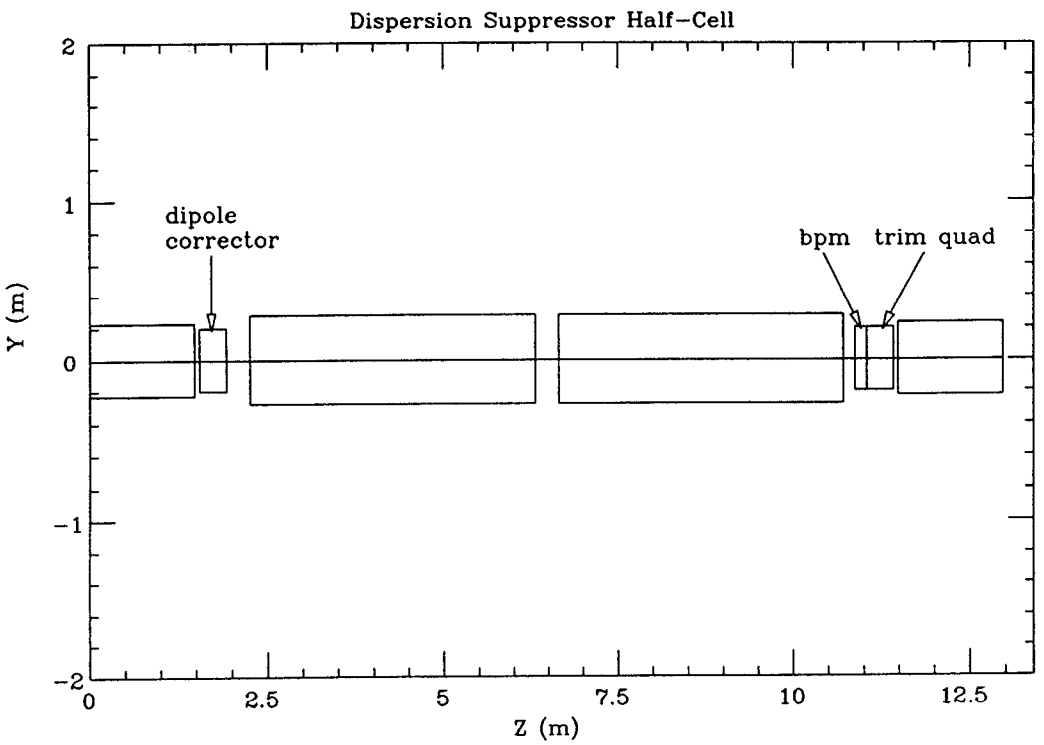
Dispersion Suppressor Half-Cell
dipole
corrector
bpm
trim quad
Y (m)
Z (m)
2
1
0
-1
-2
0
2.5
5
7.5
10
12.5

Figure 1

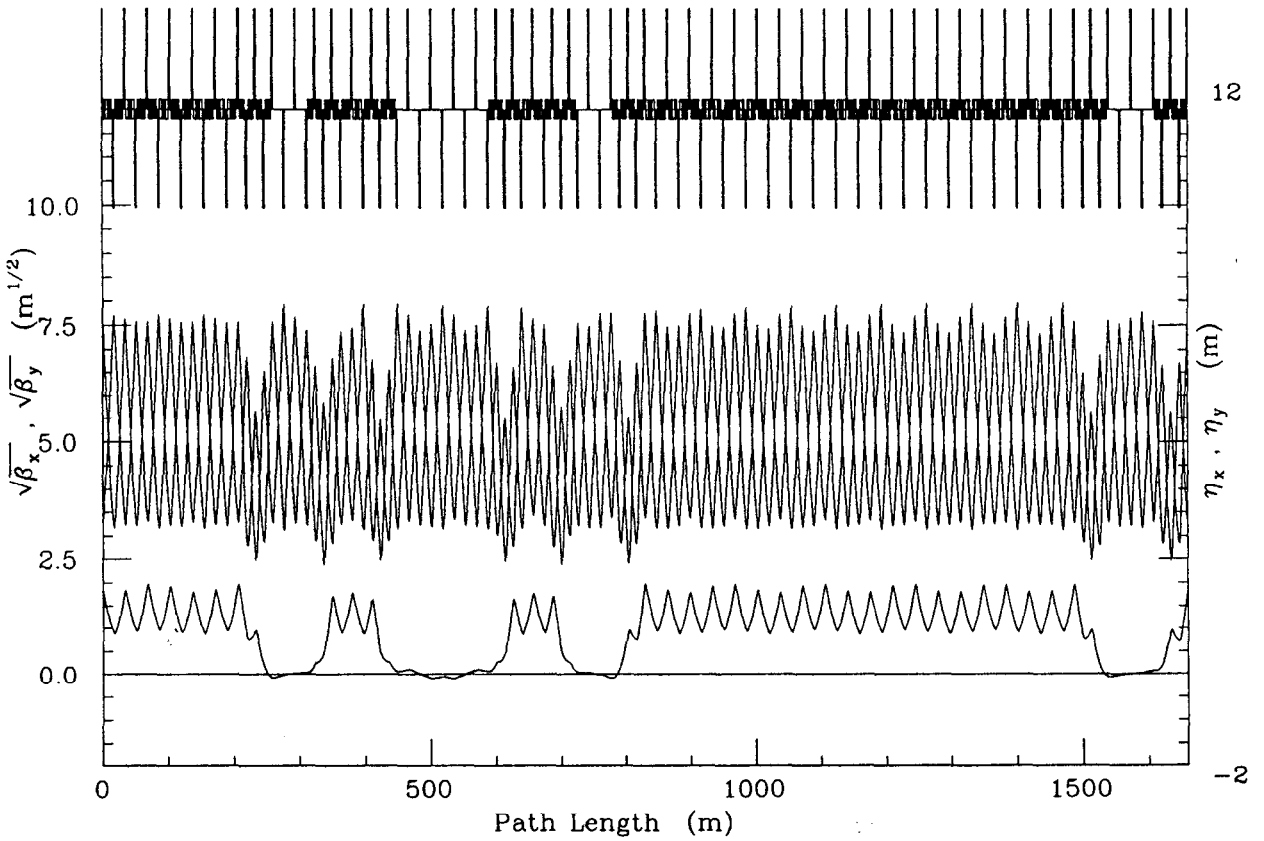
12
10.0
7.5
5.0
2.5
0.0
$\sqrt{\beta_x}$, $\sqrt{\beta_y}$ (m$^{1/2}$)
η_x , η_y (m)
−2
0
500
1000
1500
Path Length (m)

Figure 2

CHROMATICITY COMPENSATION

In addition to the dipoles and quadrupoles the Main Injector lattice includes two families of sextupole magnets (focusing and defocusing) located in the regular cells adjacent to the respective quadrupoles. The integrated strength, S, of an individual sextupole of length L (in geometric units of m^{-2}) is introduced as follows

$$\Delta x' = -\left(\int_0^L s\, dl\right) x^2 = S\, x^2 \qquad (2)$$

There is also additional sextupole field induced by each dipole magnet. This field combines the effect of eddy current as well as sextupole saturation and static sextupole field. For the purpose of our calculation these effects can be implemented by inserting a zero-length sextupole at the middle of each dipole. The integrated strength of the sextupole is expressed in terms of various contributions to the sextupole field as follows

$$S_e = \theta_{dip}\, b_2^{tot} \quad , \qquad (3)$$

where b_2^{tot} contains the above mentioned contributions to the dipole sextupole

$$b_2^{tot} = b_2^{edd} + b_2^{sat} + b_2^{sta} \, , \qquad (4)$$

and θ_{dip} is the bend angle of the dipole magnet.

The goal of this two families of sextupoles (f and d) is to compensate the natural chromaticity, $\underline{\chi}^o$, in the presence of the dipole sextupole, S_e, to some desired value, $\underline{\chi}$, (both in the horizontal and vertical

planes). One can describe the above compensation scheme in the following convenient notation (in terms of six sensitivity coefficients)

$$\underline{\chi} = \underline{\chi}^{o} + S_e \underline{e} + \mathbf{M} \begin{pmatrix} S_f \\ S_d \end{pmatrix} \tag{5}$$

Here, the underlined symbols denote 2-dim column vectors and the bold face characters represent two-by-two matrices. These two dimensional objects correspond to the horizontal and vertical degrees of freedom, respectively. One can easily identify the six sensitivity coefficients with the components of $\underline{e}$ and **M**.

It is useful to express the sextupole strength in magnetic units of Tesla/m. Therefore, we introduce a column vector strength, $\underline{g}$. Its components describe the sextupole strength of both families (f and d) as follows

$$\underline{g} = (B\rho) \begin{pmatrix} S_f \\ S_d \end{pmatrix} \tag{6}$$

Solving Eq.(5) with respect to $\underline{g}$ and applying Eqs.(3), (4) and (6) yields the following formula

$$\underline{g} = (B\rho)\, \mathbf{M}^{-1} [\underline{\chi} - \underline{\chi}^{o} + \theta_{dip}\, b_2^{tot}\, \underline{e}\,] . \tag{7}$$

The above expression will be used to analyze the required sextupole strength as a function of changing B-field along two basic Main Injector ramps for different chromaticity compensations. The sensitivity coefficients for three families of sextupoles, $\underline{e}$ and **M**, are simulated for the mi_17 lattice using MAD (version 8.71) tracking code[1]. The resulting coefficients along with the natural chromaticity, $\underline{\chi}^{o}$, are listed below

$$\mathbf{M} = \begin{pmatrix} 8.28 & 0.901 \\ -1.82 & -4.43 \end{pmatrix} \times 10^2,$$

$$\underline{e} = \begin{pmatrix} 1.59 \\ -1.49 \end{pmatrix} \times 10^3, \tag{8}$$

$$\underline{\chi}^o = \begin{pmatrix} -33.6 \\ -32.9 \end{pmatrix} .$$

To complete the sextupole strength analysis, outlined by Eq.(7), one has to gain some insight into the sextupole content of a dipole magnet and its variation with B-field. This will be discussed in detail in the next section.

SEXTUPOLE CONTENT OF A DIPOLE MAGNET

First, we consider the sextupole field induced by the eddy current flowing in the Main Injector dipole magnet lamination. Assuming that the field is proportional to the eddy current density, which in turn is linear in $\dot{B}_o$ one gets immediately the following simple relationship

$$b_2^{edd} = 8.128 \times 10^{-2} \frac{\dot{B}_o}{B_o} \quad [m^{-2}] , \tag{9}$$

Here, the numerical proportionality coefficient was found elsewhere[2] through numerical simulations.

Combined contributions of the saturation and static sextupole fields was found experimentally[3] via the flat coil measurement of the dipole magnet. The resulting sextupole strength variation with B-field is illustrated in Figure 3. One can parametrize this dependence through the following polynomial fit

$$b_2^{sat} = a_1 + a_2(B_o^4 - B_o^5) \quad [m^{-2}] , \tag{10}$$

where

$$a_1 = 6.731 \times 10^{-2} ,$$

$$a_2 = 2.569 \times 10^{-1} .$$

Further analysis of the sextupole strength will be carried out in parallel fashion for two realistic Main Injector ramps[4], namely the 150 GeV "standard ramp" and the 120 GeV "slow spill ramp". Corresponding plots will be labelled accordingly. The B-field and its time derivative as a function of time are illustrated in Figure 4. To summarize the dipole content of the sextupole field as it evolves in time we evaluate Eqs.(9) and (10) along both ramps given by Figure 4. The resulting saturation and eddy current sextupole strengths

histories are plotted in Figure 5. As one may have expected, the dipole sextupole at low B-fiels starts at some static plateau and it is virtually dominated by the eddy current sextupole, while at higher B-fields the saturation components picks up and it eventually shapes up the sextupole field profile at the end of a ramp.

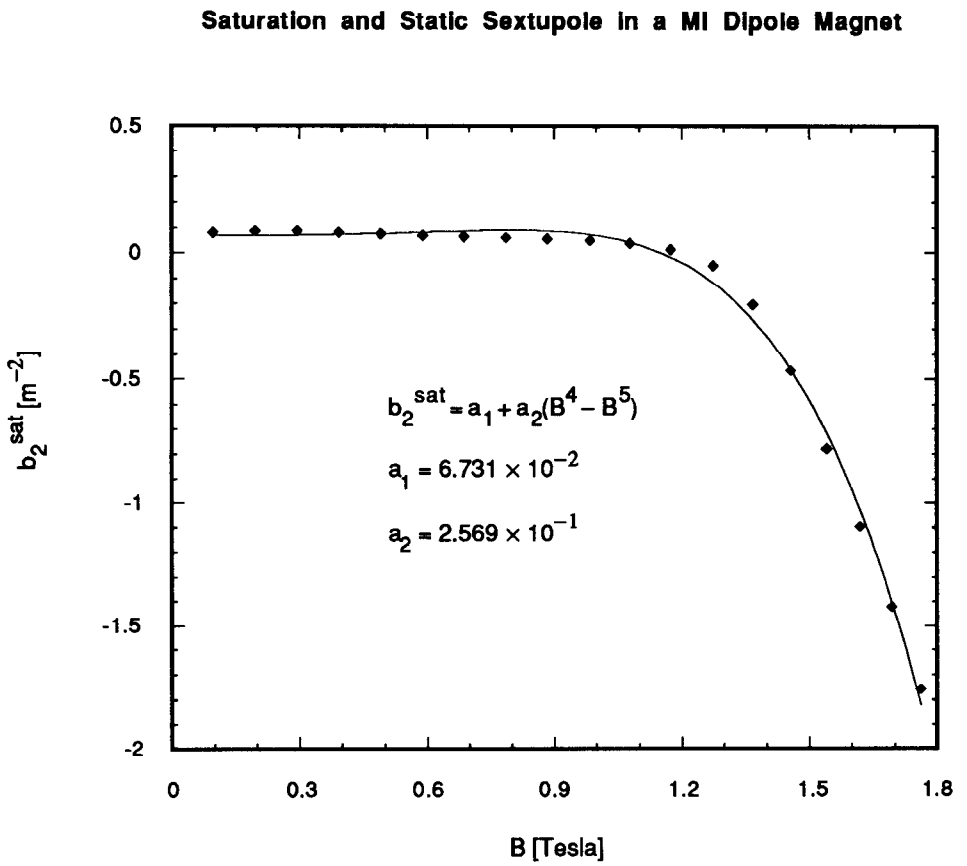

Figure 3

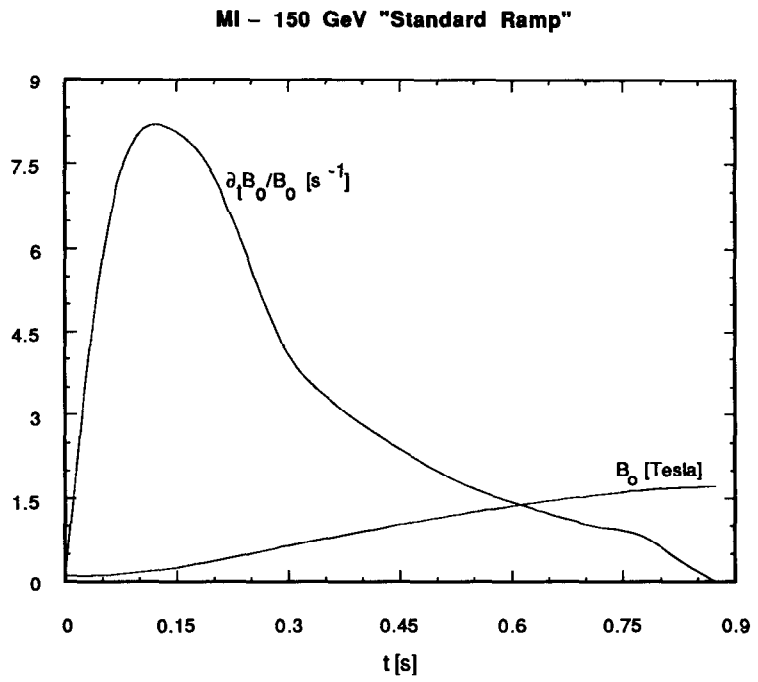
MI – 150 GeV "Standard Ramp"
9
7.5
6
4.5
3
1.5
0
$\partial_t B_0/B_0$ [s^{-1}]
B_0 [Tesla]
0
0.15
0.3
0.45
0.6
0.75
0.9
t [s]

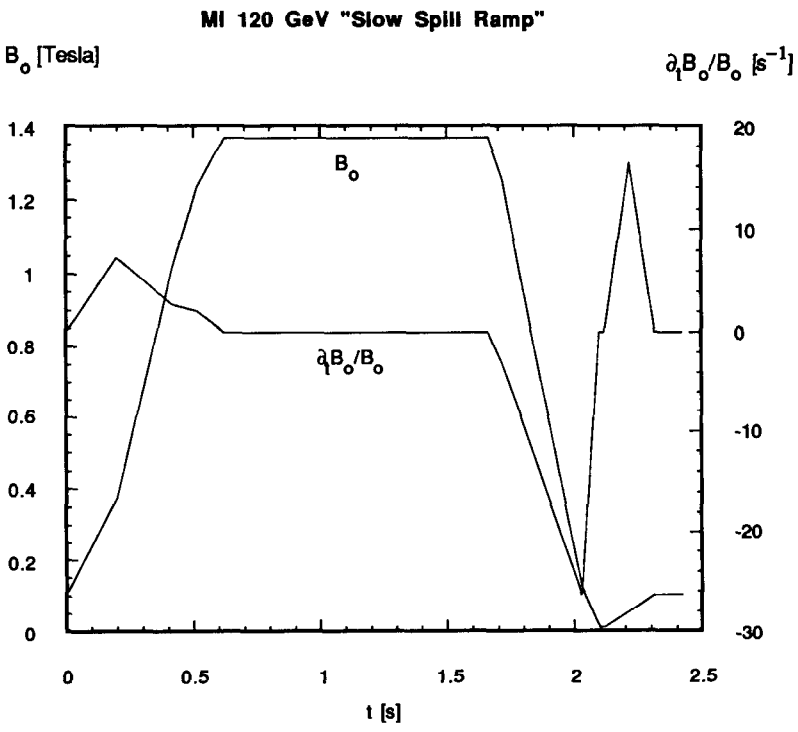
MI 120 GeV "Slow Spill Ramp"
B_0 [Tesla]
$\partial_t B_0/B_0$ [s^{-1}]
1.4
1.2
1
0.8
0.6
0.4
0.2
0
20
10
0
-10
-20
-30
B_0
$\partial_t B_0/B_0$
0
0.5
1
1.5
2
2.5
t [s]

Figure 4

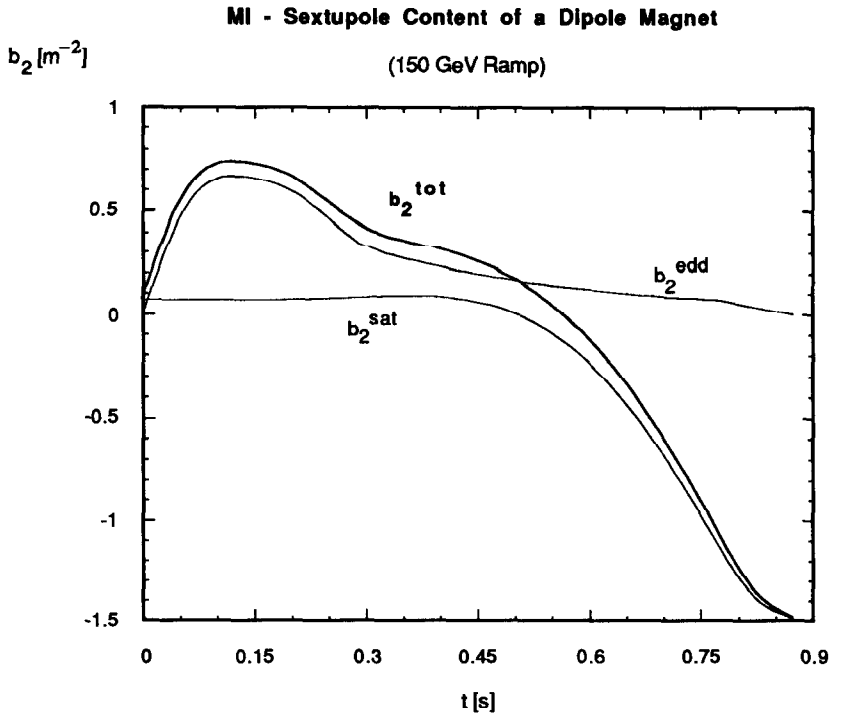
MI - Sextupole Content of a Dipole Magnet
(150 GeV Ramp)
b2 [m−2]
b2 tot
b2 edd
b2 sat
1
0.5
0
-0.5
-1
-1.5
0
0.15
0.3
0.45
0.6
0.75
0.9
t [s]

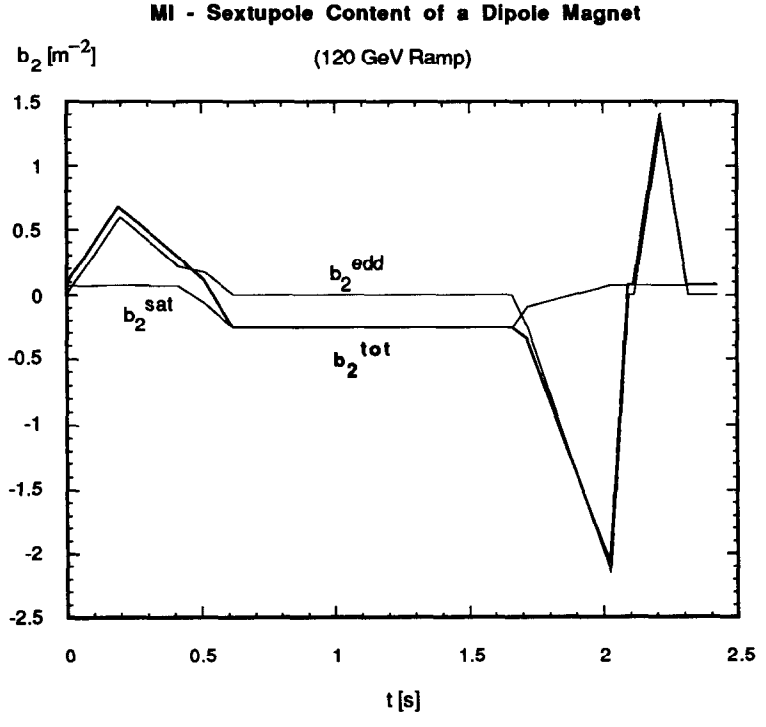
MI - Sextupole Content of a Dipole Magnet
(120 GeV Ramp)
b2 [m−2]
b2 edd
b2 sat
b2 tot
1.5
1
0.5
0
-0.5
-1
-1.5
-2
-2.5
0
0.5
1
1.5
2
2.5
t [s]

Figure 5

SEXTUPOLE STRENGTH – CONCLUSIONS

Now, one can evaluate the correcting sextupole strength, $\underline{g}$, given by Eq.(7), for each value of b_2^{sat} taken from Figure 5. This procedure will generate sextupole strength ramps for both families of correcting sextupoles (f and d). Figure 6 summarizes final sextupole requirements for various chromaticity compensations, namely the chromaticity flip at transition (from -20 chromaticity units before transition to 20 units above transition) and zero chromaticity maintained throughout the whole ramp.

As one can see from Figure 6, the extreme value of the defocusing sextupole strength is bound by 60 Tesla/m for both ramps, while the maximum required strength of the focusing family in case of the regular 150 GeV ramp (70 Tesla/m) is much higher than the corresponding strength for the slow spill 120 GeV ramp (35 Tesla/m). This last feature is a result of smaller saturation sextupole component in case of the slow spill ramp (see Figure 5).